Diffusion and Defect Forum Vols. 53-54 (1987) pp 213-226

doi:10.4028/www.scientific.net/DDF.53-54.213

Diffusion and Defect Data Vol. 53-54 (1987) pp. 213-226

INFLUENCE OF PROCESSING PARAMETERS ON THE DEFECT STRUCTURES OF GEL-DERIVED SILICAS

D.L. Griscom (a) and C.J. Brinker (b)

(a) Naval Research Laboratory, Washington, DC 20375, USA
(b) Sandia National Laboratories, Albuquerque, NM 87185, USA

ESR methods have been used to elucidate the types and relative yields of defect centers induced in sol-gel silica glasses by 100 keV x rays at 77 K in relation to the type of solvent employed in the hydrolysis step and the temperatures and atmospheres of post-gellation heat treatments. In general, glasses experiencing anneal temperatures ≤600 C exhibit >10 times more defects for a 10-MRad dose than do specimens annealed to ≥1050 C. This "excess" defect yield appears to be surface related and is shown to comprise adsorbed O_2^- and/or peroxy radicals, nonbridging-oxygen hole centers, organics, and a possible trioxide radical.

1. INTRODUCTION

Unlike the case for conventionally prepared amorphous silicon dioxide (a-SiO_2), the structure of gel-derived silica evolves sequentially as the product of a series of hydrolysis and condensation reactions and the reverse reactions, esterification, and alcoholic or hydrolytic depolymerization:

$$\equiv Si\text{-}OR + H_2O \rightleftharpoons \equiv Si\text{-}OH + ROH, \quad (1)$$

$$\equiv Si\text{-}OR + HO\text{-}Si\equiv \rightleftharpoons \equiv Si\text{-}O\text{-}Si\equiv + ROH, \quad (2)$$

$$\equiv Si\text{-}OH + HO\text{-}Si\equiv \rightleftharpoons \equiv Si\text{-}O\text{-}Si\equiv + H_2O, \quad (3)$$

where R represents an alkyl group. In solution, the above reactions lead to gelation. Subsequent solvent evaporation results in high-surface-area solids (~1000 m^2/g) whose surfaces are terminated with OH or OR groups, the concentrations of which depend on $H_2O/Si(OR)_4$ molar ratios, the concentration of ROH, the specific catalytic conditions, etc. [1-3]. During the heat treatments employed for condensation, organic substituents are volatilized or pyrolyzed at temperatures below ~450 C. Silanols continue to condense according to Eq. (3) throughout the complete course of consolidation. Prolonged heating to ~1000 C results in a fully dense material which is difficult to distinguish from conventional melt silicas [4].

Previous Raman [2,3], DSC [2,3], and ^{29}Si NMR [4] experiments have shown that a prominent siloxane condensation product which forms at intermediate temperatures is a strained, cyclic trisiloxane "defect" characterized by a reduced Si-O-Si bond angle (viz. 137°, as compared with the average angle in a-SiO_2, ~150°).

Radiation-induced defect centers in gel-derived silicas have been previously investigated by electron spin resonance (ESR) techniques as functions of drying and consolidation. Kordas et al. [5] found peroxy-radical defects (structures of the type RO_2•, where R represents an unspecified radical or part of the glass structure) to be almost ubiquitous features of γ-irradiated sol-gel silicas in various stages of consolidation. Curiously, however, our own ESR study [6] revealed nonbridging-oxygen hole centers (NBOHCs) but no peroxy radicals following low-temperature x irradiation. In the latter work, we synthesized ^{17}O-enriched samples using $H_2{}^{17}O$ and an aprotic solvent, tetrahydrofuran (THF), to minimize isotopic dilution by esterification and/or alcoholic depolymerization according to the reverse reactions of Eqs. (1) and (2). We employed a dry O_2 atmosphere during solvent evaporation and consolidation to avert possible hydrolysis and hydrolytic depolymerization by non-^{17}O water according to Eq. (1) or the reverse of Eq. (3). We speculated in Ref. [6] that these procedures, particularly the use of THF as a solvent, might cryptically account for our previous failure to detect peroxy radicals. The present study was undertaken to clarify these issues.

We describe below our investigations of the effects of solvent type (THF versus ethanol), solvent concentration, drying and consolidation atmospheres (dry O_2 versus ambient air), and consolidation temperature on the types and relative yields of x-ray-induced defect centers in gel-derived silicas. The present report emphasizes the results pertaining to the oxygen-associated defect centers (NBOHCs and peroxy radicals); the organic radical species which we observed have been discussed in Ref. [6].

2. EXPERIMENTAL DETAILS

Samples were prepared by hydrolysis of tetraethoxysilane (TEOS) in either ethanol or THF. Specifically, THF or ethanol, TEOS, and 1M HCℓ were mixed in volume ratios of 500:100:1 ("dilute") or 100:100:1 ("concentrated") and exposed to a saturated atmosphere of H_2O at 25 C. After 96 h, 1/10 volume ratio of 0.5M NH_4OH was added. The solutions were then transferred to 7-mm-dia teflon tubes where gellation occurred in 24 h. Due to precalculated shrinkage, the gelled samples were in the form of cylinders slightly less than 3 mm in diameter. These were then heated in a gradient furnace in a flowing atmosphere of either dessicated O_2, dry N_2, or undried ambient air according to a temperature-time profile described in [6], with final 2-h holds at 250, 600, or 800 C. They were next transferred under dry N_2 to 3-mm-dia fused silica sample tubes which were evacuated by a roughing pump and sealed under vacuum. All subsequent handlings and irradiations by 100-keV x rays were carried out with the samples so encapsulated, thus obviating the adsorption of spurious gas molecules at later stages in the experiment. Defect centers induced in the tubes were annealed out with a hydrocarbon-oxygen torch while carefully maintaining the sample (at the opposite end of the tube) at the irradiation temperature of 77 K. These samples will be specified in the text by a two-letter code representing the solvent type ("E" for ethanol or "T" for THF) and whether or not the solution was dilute or concentrated ("D" or "C"), followed by a number specifying the final anneal temperature in degrees C. Thus, for example, the designation "ED-600" represents a sample hydrolized in a dilute ethanol solution and annealed at 600 C. Unless further specified by appending "air" or "N_2", the anneal atmosphere should be understood to be dry O_2.

The ^{17}O-enriched samples (see Ref. [6]) were all of the "TD" type. Two of these were reheated to 1050 and 1200 C in a gradient furnace in dry flowing O_2. In the course of these reheatings, the viscosities of the samples were dramatically lowered, causing them to break up into droplets. Thus, the samples designated TD-1050 and TD-1200 were in the form of coarse powders which were encapsulated in silica tubes and otherwise handled as described above. Unfortunately, the overall ^{17}O enrichment of these samples was inadvertently diluted when they became blended with an unenriched sol-gel material (prepared in the same manner) which was used as a support in the furnace.

Some preliminary studies were carried out on a base-catalyzed gel (sample B2 of ref. [1]) which was annealed in air to 650 C, handled in ambient air, and irradiated "naked" in contact with the liquid nitrogen bath. This sample will be designated in the text simply as "B2".

ESR spectra were obtained on a Bruker ER 200 instrument operating at 9.4 GHz with the sample temperature maintained at 110 K by means of a nitrogen flow-through accessory. In situ isochronal anneals were accomplished by varying the temperature of the N_2 stream.

3. EXPERIMENTAL RESULTS AND DISCUSSION

3.1 Preliminary results and background

Figure 1 illustrates the ESR spectrum of "naked" sample B2 x irradiated at 77 K. (The particular line shape seen here was obtained after the sample had been subjected to two previous low-temperature irradiations and rewarmed each time to room temperature; a somewhat different line shape was observed initially.) The many "bumps" seen to the low-field side of the derivative zero-crossing are here interpreted as corresponding to the g_3 values of a sequence of O_2^- ions in differing crystal-field environments and/or several peroxy radicals, ROO•. In either case, the various g_3 values would be mathematically related to differing splittings Δ of the $2p\pi$ antibonding orbital of the oxygen-oxygen homobond (see, e.g., Refs. [7] or [8]). To test this O_2^-/peroxy-radical interpretation, we used the measured g_3 values in conjunction with the theory of Känzig and Cohen [7] to calculate Δ and thence the values of g_2 and g_1 indicated by the "combs" drawn on Fig. 1. In turn, these g values were used to effect the computer line-shape simulation represented by the dashed curve. On the basis of this successful simulation, we suggest that the entire spectrum (with the possible exception of a narrow component located near the zero-crossing) is due to O_2^- ions or peroxy radicals in at least five distinguishable chemical environments. (This interpretation is similar to one offered by Kordas et al. [5] to explain a somewhat different spectrum observed at room temperature in a γ-irradiated sol-gel silica -- although these workers did not buttress their case with a computer simulation.)

An isochronal anneal experiment showed the putative O_2^- species of the present study to decay at distinctly differing rates, with the three bumps at $g \leq 2.04$ disappearing after a 7-min anneal at 140 K and the peak at $g \approx 2.05$ vanishing at 240 K (thus ruling out the possibility that the four equally spaced "g_3 bumps" may comprise a hyperfine quartet). Only the component with a g_3 value of ~2.07 survived warming to room temperature, at which point the overall intensity had fallen to ~1 % of its initial value at 110 K. The thermal instability of these defects induced by x rays at cryogenic temperatures distinguishes the present study from those of Kordas et al. [5] who studied room-temperature-stable species induced by an unspecified γ-ray dose at 300 K.

The well known E' center (≡Si•) [9] was also detected in sample B2 and the other samples of this study, but in all cases its intensity was found to be ~10 to 500 times weaker than those of the oxygen-related species or organics. For this reason, the E' center will not be further discussed in the present article.

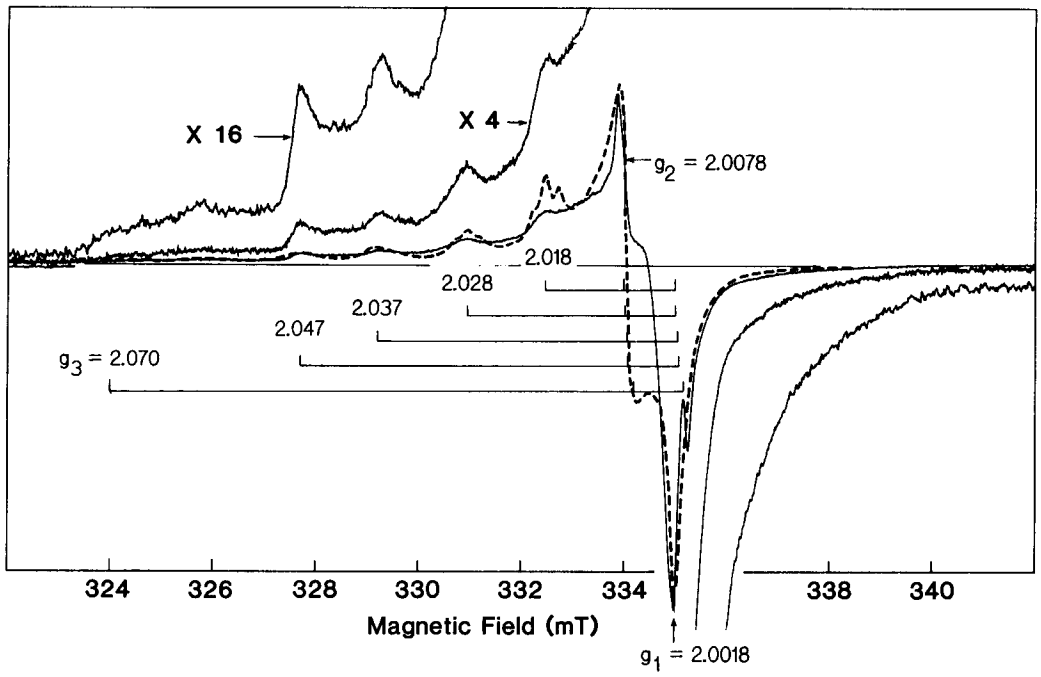

Fig. 1. ESR spectrum of sample B2 recorded at 100 K following a 5.5-MRad x irradiation at 77 K (microwave power 28 dB). The dashed curve is a computer simulation based on an O_2^- model: five individual component spectra corresponding to the five g-value "combs" were added together in the ratios 1:1:1:1:1. A narrow distribution of g_3 values was assumed for each component; (the multi-peak structure centered on g=2.018 is an artifact of this procedure).

Figure 2 reproduces from our earlier paper [6] the broad-field-scan spectrum of the ^{17}O-enriched sample TD-600-N_2 exposed to a 15.5-Mrad x irradiation at 77 K and briefly warmed to 130 K to attenuate a pair of lines due to atomic hydrogen. As described in Ref. [6], the dashed computer simulation was accomplished by using g values (distribution in g_3 values illustrated in inset) and hyperfine coupling constants ($A_{\|}$=11.0 mT) typical of nonbridging-oxygen hole centers [10]. The absence of identifiable hyperfine lines due to O_2^- ions or peroxy radicals was a puzzle which was addressed in the new experiments described below.

3.2 Where are the peroxy radicals?

In Ref. [6] we suggested that the presence or absence of peroxy radicals in irradiated sol-gel silicas might be a function of processing conditions. However, as will be described below, the apparent absence of O_2^-/peroxy radicals in the spectrum of Fig. 2 is largely an effect of the experimental conditions selected to maximize the signal to noise ratio of the ^{17}O hyperfine lines.

Figure 3 illustrates the influence of microwave power level on the ESR spectra of sample TC-600 subjected to 13.5 Mrads 100-keV x irradiation at 77 K. At low powers (48 - 54 dB), one observes the presence of E' centers and a resonance with the appropriate g_2 value for peroxy radicals. At higher powers,

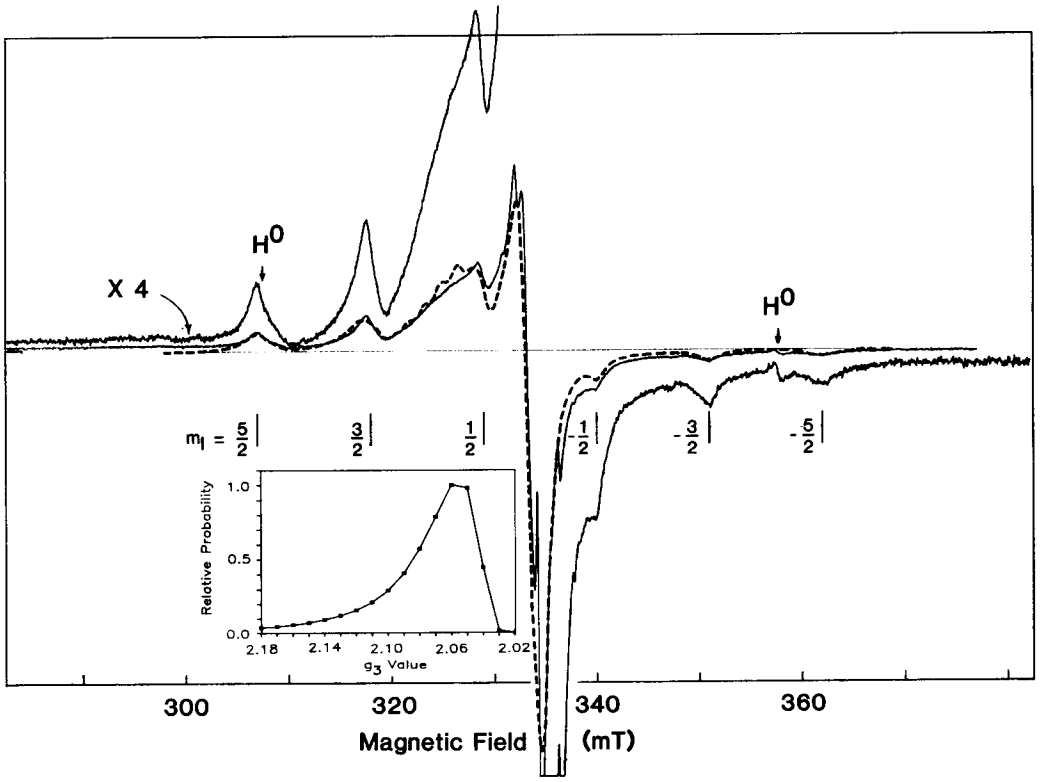

Fig. 2. Broad-field-scan, high-microwave-power (6 dB) ESR spectrum of ^{17}O-enriched sample TD-600-N_2 recorded at 105 K following 15.5-MRad x irradiation at 77K. Dashed curve is a computer simulation as described in the text and Ref. [6]. Six ^{17}O hyperfine lines are indicated by their nuclear magnetic quantum numbers m_I.

increasingly large signals are observed due to NBOHCs (as indicated on the figure) and organic radicals (e.g., the sharp lines and shoulders located to the high-field side of the E' center). (The reader should consult Ref. [6] for an analysis of the lines due to organics.) Figure 3 shows clearly that a power level of 6 dB begins to favor the contribution of the NBOHC over that of the peroxy radical which it overlaps.

Figure 4 exhibits some significant effects of accumulated x-ray dose on the ESR spectrum of sample TD-600. Here, it can be seen that the g_3 "bumps" and the g_2 zero-crossing near 2.0070, both associated with O_2^-/peroxy radicals, are maximized at a dose near 4.5 Mrads and decrease sharply when the accumulated dose is increased to 13.5 Mrads. Thus, the 15.5-Mrad dose employed in obtaining the spectrum of Fig. 2 is seen in retrospect to have been an inappropriate condition for maximizing the yield of O_2^-/peroxy-radical species.

The sharp resonance in Fig. 4a with a zero-crossing near g=2.0042 has not been previously reported in irradiated sol-gel silicas. Comparing the g values of this narrow feature with the literature [11,12] leads to its tentative identification as arising from a trioxide radical, ROOO•. The presence of this apparently unstable intermediate species may be the source of the discrepancy between the experimental and computed spectra of Fig. 1.

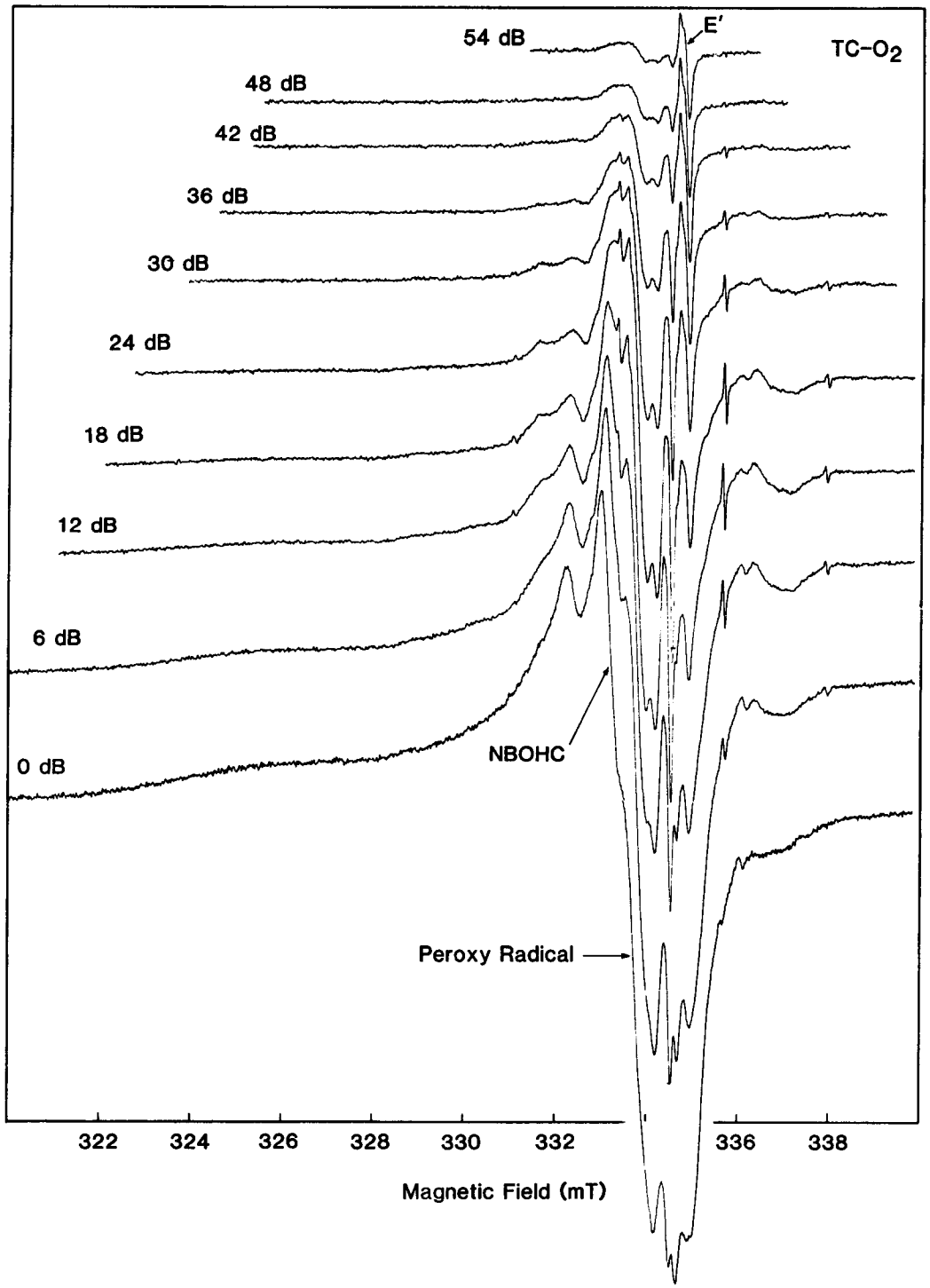

Fig. 3. Effect of microwave power saturation on the ESR spectrum of sample TC-600 following 13.5-MRad x irradiation at 77 K. Data acquired at 110 K.

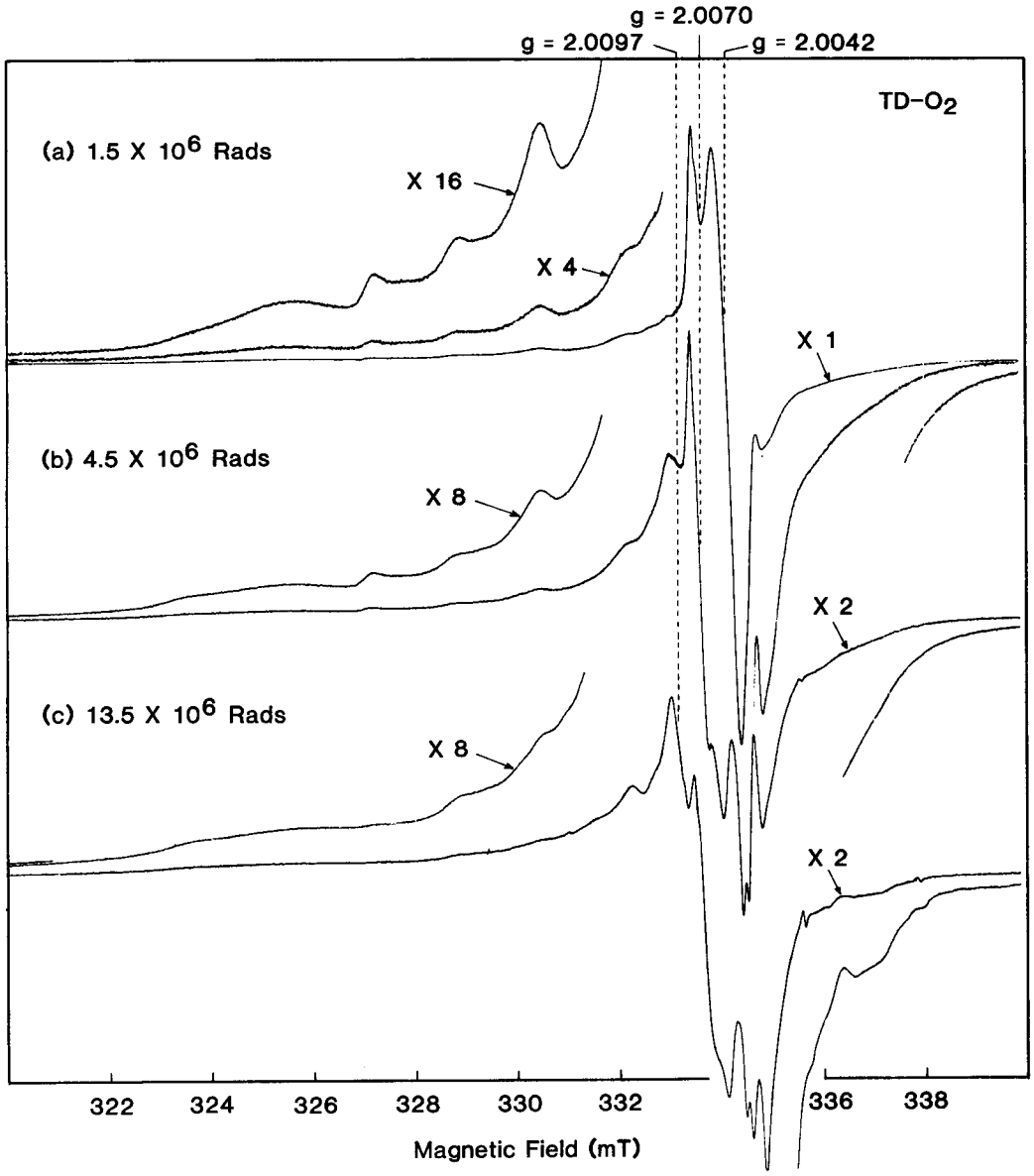

Fig. 4. Effects of cumulative x-ray dose on the ESR line shape of sample TD-600. Irradiations were performed at 77 K, measurements at 110 K (power 16 dB).

On the basis of the spectra of Figs. 3 and 4, it is now clear that the experimental conditions of Fig. 1 were ideal for resolving O_2^-/peroxy-radical spectra. But, as evident in Fig. 5, these same conditions lead to mediocre signal-to-noise ratios when searching for ^{17}O hyperfine structure. Nevertheless, the spectrum of Fig. 5, pertaining to ^{17}O-enriched sample TD-600-N_2, reveals in addition to the 11.0-mT hyperfine set of the NBOHC a weak set of

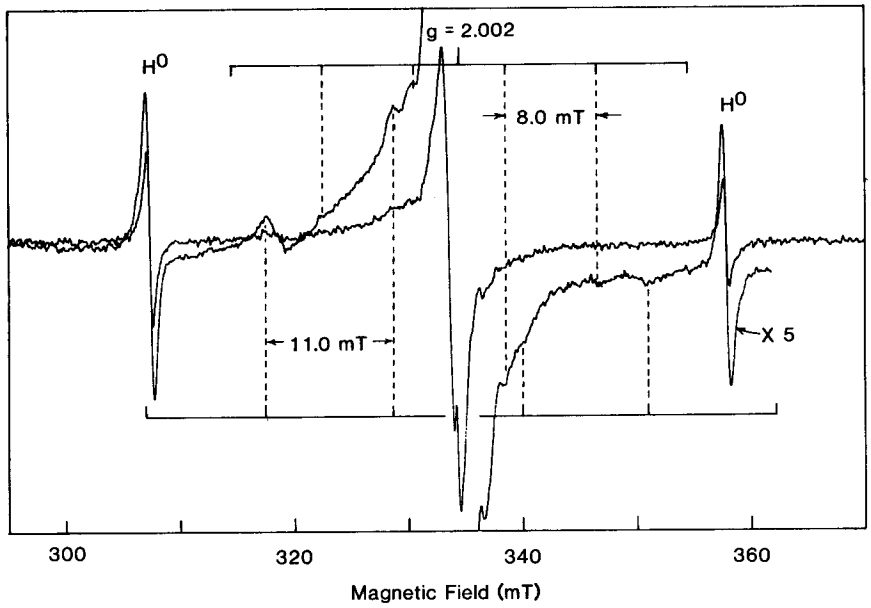

Fig. 5. ESR spectrum of ^{17}O-enriched TD-600-N_2 obtained under favorable conditions for observation of O_2^--type species (dose 4.25 MRads, power 28 dB). Combs locate hyperfine multiplets due to NBOHCs (lower) and adsorbed O_2^- (upper).

four peaks centered on g≈2.002 with a splitting of ~8.0 mT. We suggest that these four lines are the M_I=3/2, 1/2, -1/2, and -3/2 hyperfine peaks of an $^{17}O^{16}O^-$ species (assuming the M_I=5/2 and -5/2 peaks to be unresolved). If this interpretation is correct, the magnitude of the hyperfine splitting is indicative of a surface-adsorbed O_2^- ion [13]. The relatively low intensities of these four lines are consistent with the fact that most of the surface-adsorbed $^{17}O_2$ molecules are likely to have come from the anneal atmosphere, which was not ^{17}O enriched. To test these interpretations, we are planning additional experiments involving adsorption of ^{17}O-enriched oxygen molecules on sol-gel silicas of natural isotopic abundance.

3.3 Effects of anneal temperature on defect stability

In Fig. 6 we present isochronal anneal data for x-ray-induced atomic hydrogen and oxygen-associated hole centers (OHCs, which may include both NBOHCs and O_2^-/peroxy radicals) in relation to the pre-irradiation anneal temperature. Other processing parameters were held constant in this experiment. (The x-ray doses were 22 MRads for the 1050- and 1200-C samples and 8 MRads for the 600- and 800-C samples). The differing anneal curves for H^0 suggest that the hydrogen atoms are trapped in differing environments in glasses processed at different temperatures. An observed monotonic decrease in the initial linewidth of the H^0 hyperfine lines with increasing pre-irradiation anneal temperature (Fig. 7) also supports such a conclusion. The data of Fig. 6b show that the OHCs become increasingly stable as the anneal temperature is raised from 600 to 1050 C, whereas the change in going from 1050 to 1200 C is small and perhaps not statistically significant.

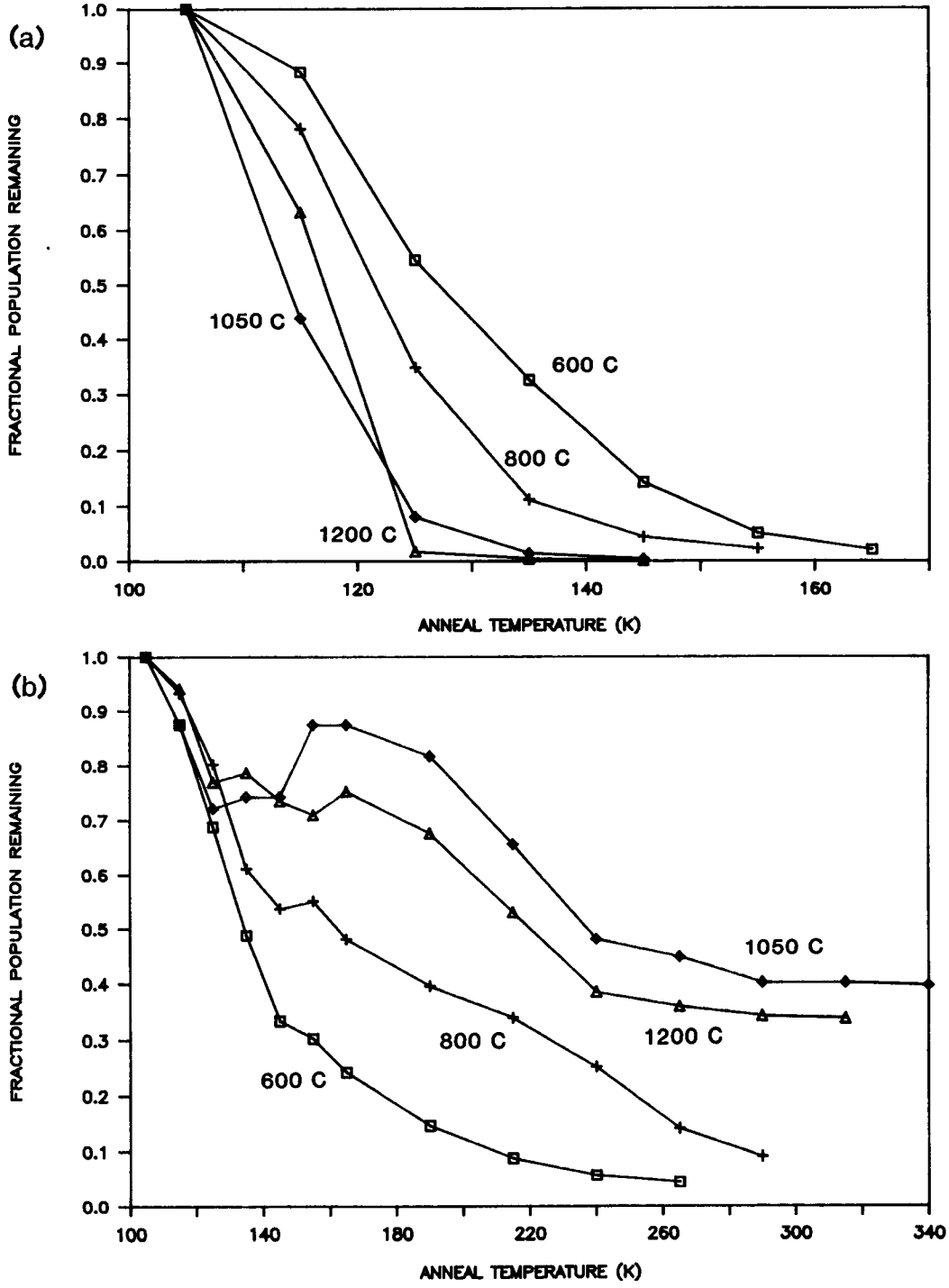

Fig. 6. Isochronal anneal curves (5 min at temperature) for x-ray-induced defect centers in sol-gel silicas annealed at various temperatures: (a) atomic hydrogen, (b) oxygen hole centers (NBOHCs plus O_2^-/peroxy radicals).

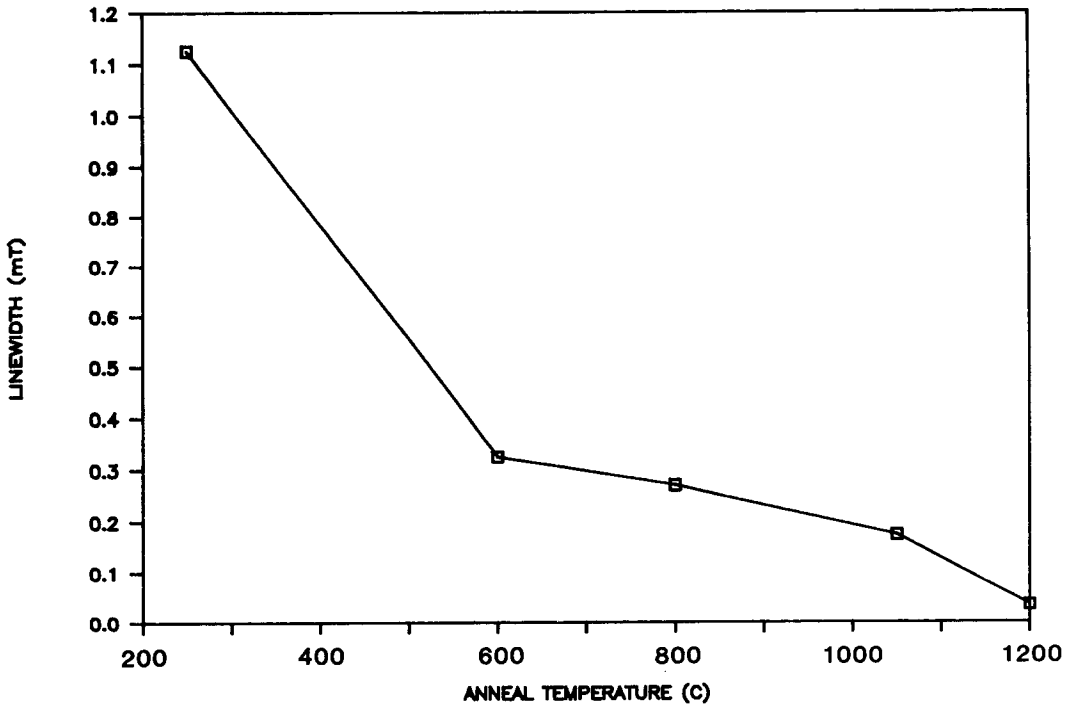

Fig. 7. Width of H^0 hyperfine lines measured at 110 K, immediately following x irradiation at 77 K. Absissa represents the pre-irradiation anneal temperature.

3.4 Influences of other processing parameters and the radiation "fatigue" effect

Absolute spin concentrations were determined by numerical integration of spectra recorded at 110 K immediately following irradiation at 77 K and comparison to a Varian strong pitch standard. The results are shown in Fig. 8 as functions of accumulated x-ray dose. Figure 8a illustrates the influence of anneal temperature on the oxygen hole center yields in "TD-type" samples, with a comparison to "ED" and "TC" glasses annealed at 600 C only. The dashed curve is included as an aid to the eye in defining a linear growth law on this log-log plot; coincidently it also represents the previously determined growth behavior and absolute concentrations of x-ray-induced OHCs in Type-III synthetic fused silicas [14]. Thus, with respect to the absolute yield of OHCs, sol-gel silicas annealed to 1050 and 1200 C are seen to behave generally the same as high-temperature melt silicas (the differing slopes of the curves for the 1050- and 1200-C samples are tentatively ascribed to signal-to-noise problems).

Figure 8b shows the growth behaviors of defects in sol-gel silicas produced by several processing routes, but with the anneal temperature for all samples being 600 C. The defects counted here are mostly OHCs in the case of the samples annealed in O_2 but include a substantial organic radical component in the case of those samples annealed in air. In fact, for samples TD-600-air and ED-600-air, the overall defect concentration comprised mainly OHCs at the lowest dose (0.15 Mrads) but mainly ethyl alcohol radicals [6,15] at the highest dose (4.0 Mrads). Careful inspection of the data revealed that the OHC population reached a maximum at an intermediate dose and then declined at the highest dose.

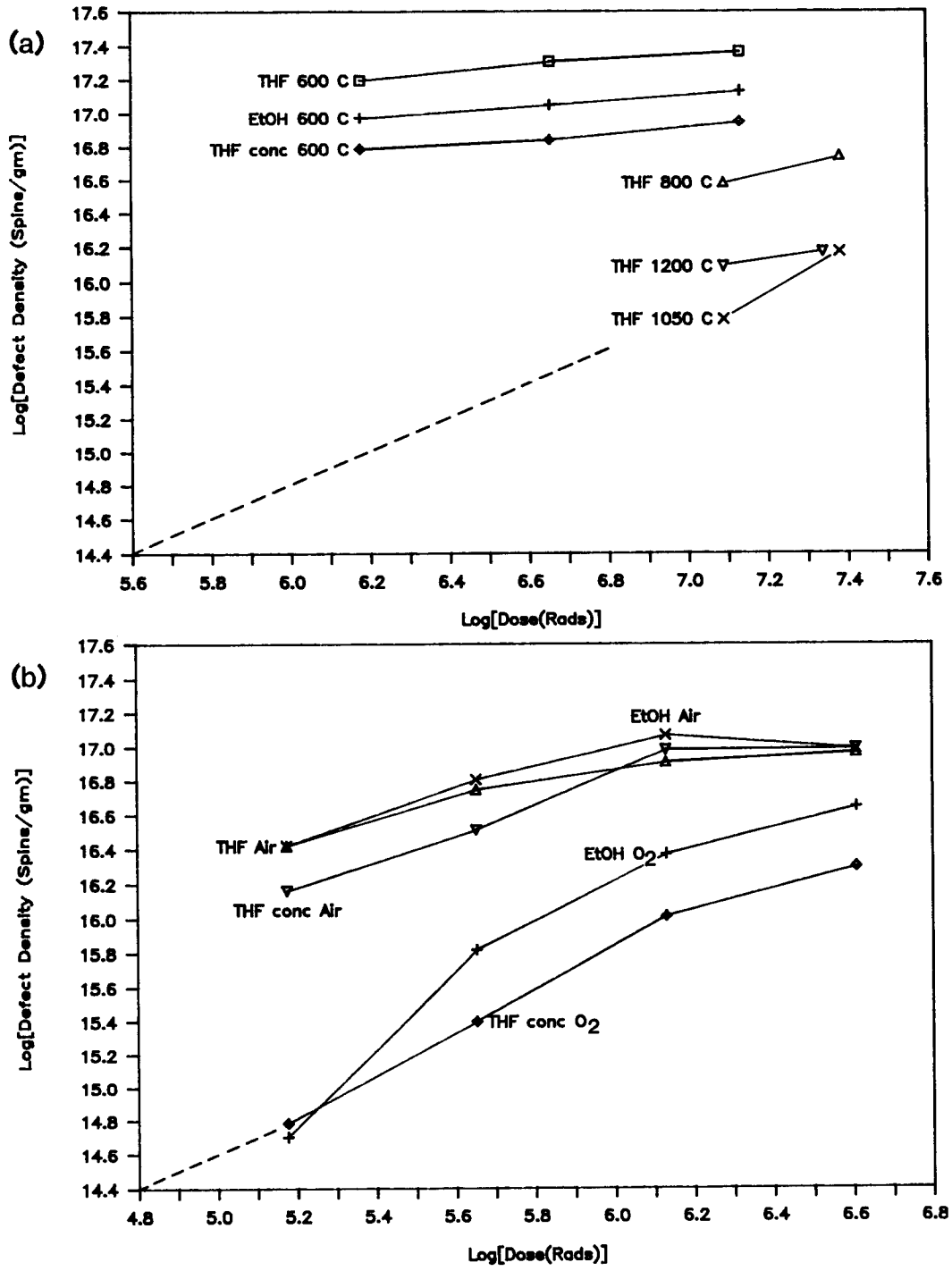

Fig. 8. X-ray-dose dependence of absolute defect concentrations in sol-gel silicas in relation to (a) anneal temperature and (b) anneal atmosphere (note different dose scales). All of the samples of (b) were annealed at 600 C.

The data for samples ED-600-O_2 and TC-600-O_2 shown in Fig. 8b were obtained after the samples had been already exposed to a 13.5-Mrad cumulative x-ray dose at 77 K (resulting in the data of Fig. 8a), thermally bleached at room temperature, and recooled. Significantly, the total defect concentrations measured in these samples at a dose of 4 Mrads is lower after the second irradiation by a factor of ~4 with respect to the corresponding yield in response to the first irradiation. We will refer to this radiolytic preconditioning effect as "fatigue".

In all of the foregoing results, no qualitative nor major quantitative differences were observed between glasses hydrolyzed in ethanol and those hydrolyzed in THF (thus obviating our speculation in Ref. [6]). Neither was there noticed a definite effect of the degree of solvent dilution. (We believe that the lower defect yields in the "TC" samples vis-à-vis the "TD" materials are due mainly to the fact that the "TC" samples broke apart in the sample tube and thus manifested lower ESR "filling factors" relative to the samples which remained solid cylinders.)

It appears that the anneal atmosphere accounts for the most profound differences in the radiation responses of the samples investigated: Figure 9 compares the line shapes observed for ED-600-air (at low dose before the OHCs were supplanted by organic radicals) and ED-600-O_2. The spectrum of the latter was essentially identical with that obtained for TC-600-O_2 at the same microwave power (Fig. 3, 6 dB). By contrast, the spectrum of ED-600-air is seen to be

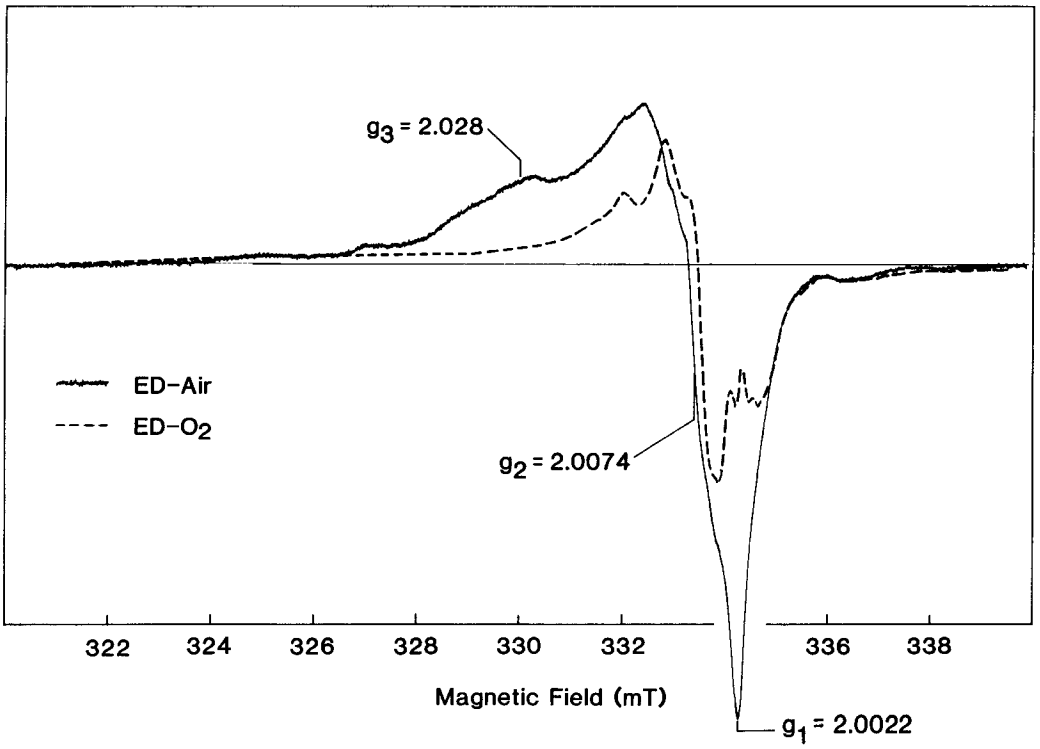

Fig. 9. Comparison of the ESR spectra of otherwise-identical sol-gel silicas annealed at 600 C in different atmospheres prior to x irradiation at 77 K. Doses were 0.15 and 4.0 MRads for the air- and O_2-annealed samples (unbroken and dashed curves, respectively). The measurement temperature was 110 K.

quite different. While displaying a qualitative similarity to the O_2^-/peroxy radical spectrum of Fig. 1, the spectrum of the air-annealed sample of Fig. 9 exhibits a greater relative prevalence of spectral components for which $g_3<2.03$. Since small values of g_3 imply large values of the crystal field splitting parameter Δ [7,11,13], a particularly strong bonding is inferred between the radical R and the O_2^- ion if the species should be of the ROO• type. Based on a comparison of the g values to the literature [11], an HOO• radical could give the observed spectral line shape. Such an identification is in consonance with the fact that a major difference between dry O_2 and ambient air is the water content. (In this context we point out that other molecular species present in air, such as nitrogen and carbon dioxide, give rise to free radicals characterized by quite different ESR line shapes [11], none of which were observed in the present experiment.) On the basis of these considerations, we propose that the ED-600-air spectrum of Fig. 9 arises largely from HOO• radicals, which may originate from the attachment of a radiolytic hydrogen atom to an adsorbed O_2 molecule.

In any event, the species responsible for the unbroken curve of Fig. 9 is evidently unstable against prolonged irradiations and is therefore best catagorized as an unstable intermediate in a reaction chain leading at high doses to the production of $CH_3\dot{C}H{\bullet}OH$ radicals [6]. We suggest here that prolonged irradiations may result in the fissioning of the $H-O_2$ bond, making additional atomic hydrogen available for the reaction [6]:

$$H^0 + CH_3{\bullet}CH_2{\bullet}OH \rightarrow CH_3{\bullet}\dot{C}H{\bullet}OH + H_2. \qquad (4)$$

We speculate further that the reaction chain may terminate with the desorption of the radiolytic molecular hydrogen appearing on the right-hand side of Eq. (4).

4. CONCLUSIONS

Figure 8 demonstrates that the overall defect yields at 77 K in the highly porous 600-C-annealed samples saturate at x-ray doses ≤1 MRad, attaining at that point numerical values one to two orders of magnitude higher than those measured for fully-dense silica glasses. Moreover, defects manifesting these enhanced spectral intensities appear to arise from radiolysis of molecular species associated with either the anneal atmosphere (e.g., O_2 or H_2O) or the products of hydrolysis (e.g., ethanol). These facts are regarded as prima-facie evidence that the "excess" defect concentrations in the porous gels are created on the internal surfaces or in the "soup" which fills the pore structure. The radiation chemistry occurring in these pores is evidently complicated. In addition to fingerprinting NBOHCs on the basis of their ^{17}O hyperfine structure, we have tentatively identified the ESR spectra of HOOO•, HOO•, and O_2^- ions adsorbed at various sites. Studies of ^{17}O-enriched samples have indicated that both NBOHCs and adsorbed O_2^- species are formed upon x irradiation at 77 K. The optimum conditions for observation of each species have been delineated. Enhanced yields of NBOHCs in the more porous samples can be attributed to radiolysis of surface hydroxyl groups [6].

A possible mechanism for the "conversion" of HOO• radicals to ethyl alcohol radicals was suggested above. In order to explain why the proposed chain of radiochemical reactions should proceed irreversibly with increasing x ray dose, we postulated the irreversible loss of radiolytic H_2 from the sample. The "fatigue" effect, whereby a sample once irradiated and warmed to room temperature exhibits lower defect yields in subsequent irradiations, may have a similar explanation. Our present study has the unique feature that all of the quantitative defect yields were determined for samples sealed under vacuum and not subjected to additional atmospheric contamination during or after irradiation.

REFERENCES

1. C.J. Brinker, K.D. Keefer, D.W. Schaefer, R.A. Assink, B.D. Kay, and C.S. Ashley, J. Non-Cryst. Solids 63 (1984) 45.
2. C.J. Brinker, E.P. Roth, G.W. Scherer, and D.R. Tallant, J. Non-Cryst. Solids 71 (1985) 171.
3. C.J. Brinker, D.R. Tallant, E.P. Roth, and C.S. Ashley, Defects in Glasses, MRS Vol. 61, F.L. Galeener, D.L. Griscom, and M.J. Weber, Ed. (Materials Research Society, Pittsburgh, PA, 1986), pp. 387.
4. R. Aujla, R. Dupree, I. Farnan, and D. Holland, (these proceedings).
5. G. Kordas and R.A. Weeks, J. Non-Cryst. Solids 71 (1985) 327; G. Kordas, Defects in Glasses, MRS Vol. 61, F.L. Galeener, D.L. Griscon, and M.J. Weber, Ed. (Materials Research Society, Pittsburgh, PA, 1986), pp. 419.
6. D.L. Griscom, C.J. Brinker, and C.S. Ashley, J. Non-Cryst. Solids (in press)., 1987.
7. W. Känzig and M.H. Cohen, Phys. Rev. Lett. 3 (1959) 509.
8. D.L. Griscom, J. Non-Cryst. Solids 31 (1978) 241.
9. R.A. Weeks, J. Appl. Phys. 27 (1956) 1376.
10. M. Stapelbroek, D.L. Griscom, E.J. Friebele and G.H. Sigel, Jr., J. Non-Cryst. Solids 32 (1979) 313.
11. P.W. Atkins and M.C.R. Symons, The Structure of Inorganic Radicals (Elsevier, Amsterdam, 1967),
12. R.W. Fessenden, J. Chem. Phys. 48 (1968) 3725.
13. J.H. Lunsford, Catal. Rev. 8 (1973) 135.
14. D.L. Griscom, M. Stapelbroek, and E.J. Friebele, J. Chem. Phys. 78 (1983) 1638.
15. A.A. Wolf, E.J. Friebele, and D.C. Tran, J. Non-Cryst. Solids 71 (1985) 345.

Effects of Modes of Formation on the Structure of Glass
10.4028/www.scientific.net/DDF.53-54

Influence of Processing Parameters on the Defect Structures of Gel-Derived Silicas
10.4028/www.scientific.net/DDF.53-54.213